Analysis and control of a non-Inverter Buck-Boost Power DC-DC Converter by State-Space Modeling and applied to PV Systems under MPPT Operation

Rafael Ribeiro de Carvalho Vaz
Federal University of Goias (UFG)
Goiania/GO, Brazil
engrafaelrcv@gmail.com

Sergio Pires Pimentel
Federal University of Goias (UFG)
Goiania/GO, Brazil
sergio_pimentel@ufg.br

Sérgio Araújo
Federal University of Goias (UFG)
Goiania/GO, Brazil
sgranato1@gmail.com

***Abstract*—This paper describes the feedback closed loop steady-space with reference input and integral action for distributed power photovoltaic systems including Maximum Power Point Tracking (MPPT). In order to validate the control proposal scheme it was applied to the non-inverter Buck-Boost DC-DC power converter. The MPPT considered was the IC algorithm. Results show how this control technique could be applied in power converters in order to regulate the output voltage. The control scheme was able to follow the reference even for dynamic demand behavior. Under MPPT conditions, the PV output voltage seeks the MPPT reference input signal maximizing the output power.**

***Index Terms*—Photovoltaic System, Control System, Power Electronics, DC-DC Power Converters, Maximum Power Point Tracking (MPPT).**

I. INTRODUCTION

The demand for electricity continues to grow worldwide. This fact demands enormous pressure on power generation systems to achieve this contingency not only from the point of view of power supply systems, but also from the quality of energy delivered to the final consumers. In Brazil, large investments have been made covering the whole generation, transmission and distribution chain in order to drain the energy of the regions with large generation potential, especially hydropower, in remote regions of the country. That investment policy requires large financial efforts and a series of irreversible environmental consequences. A possible solution in order to mitigate such efforts could be the investment on Distributed Generation (DG) from alternative power sources.

The actual adoption of GD gained a great ally in the development and implementation of Smart Grids, which without it would not be possible to implement secure and fast operational solutions that can ensure a minimum level of quality and reliability to the distribution networks.

Due to a high solar irradiance rate in Brazil, with annual average around 5 kWh/m²day [1], there is great potential for adding solar power conversion into electrical energy through photovoltaic panels. However, with the currently used technology, this conversion has low efficiency revolving around 16% [2]. In order to maximize the available generation resources, there are several techniques to extract the maximum power of the photovoltaic generation system as tracking maximum incidence of solar radiation [3] and maximum power point tracking (MPPT) systems in PV panels [4].

This paper proposes an output voltage control system on DC-DC power converters. The control technique could be used in several industrial applications as charging systems, regulated sources and others. In this paper, it is applied in grid-tie photovoltaic generation systems considering power maximization techniques in such generators.

The power control strategy involves a state-space model of the power generation plant by means of the DC-DC power convert. A voltage target is set to be followed by power converter. In order to do this task the state-space control with integral action technique is applied.

In order to operate the power plant under MPPT conditions the Incremental Conductance (IC) algorithm is applied to regulate the PV output voltage. The model is tested in a 0.38/13.8kV distribution grid model. The environments characteristics as solar irradiance and cell temperature are also evaluated.

II. PHOTOVOLTAIC POWER SYSTEM

One of the issues about solar energy conversion into electricity in a photovoltaic system is related to the operation of photovoltaic or solar cells. The power output of a cell is proportional to its surface area and depends on the intensity of solar radiation and its temperature [2]. The cells can produce electricity for about 30 to 50 years old and in a few years are capable of delivering the amount of energy used in its construction. For power generation applications, it is considered a 25 years life cycle [2]. Some factors that impact the behavior of the solar cells are the temperature, the air mass and the solar irradiance.

In photovoltaic arrays, the relationship between the outputs current, I, and voltage, V, unlike a common resistor for example, is nonlinear. In the I-V curve, a point that stands out is precisely

978-1-4673-6605-2/15/$31.00 ©2015 IEEE

the one in which the product of voltage and current in module output terminals results in the maximum power supplied. These voltage value, V_{MPP}, and current value, I_{MPP}, resulting in a single point called the Maximum Power Point (MPP) from that photovoltaic array.

However, due to the dependence of the power supplied with cell temperature and irradiance on it, even for a fixed point on the surface of the earth, this operating point is not constant. Figure 1 illustrates the behavior of operation point with the variation on the cell temperature and solar irradiation.

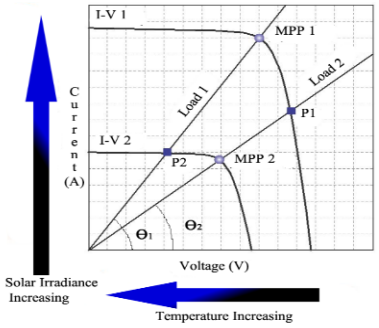

Figure 1.Effects on curver V-I of solar cells considering increases of temperature (to left) and irradiance (to up).

As can be seen at Figure 1 the Load1, with I-V1 and MPP1 initial conditions, changes its operation point to the I-V2 characteristic by either decrease of irradiance or increase in temperature and relies on P2. This is not the MPP for that condition (I-V2), which is on MPP2. The same occurs with I-V2 when the cell temperature either decreases or increases the solar irradiance. Note that for changing its operating point to MPP2, a new load angle θ (load curve) must be adopted.

A lot of MPPT techniques for this purpose have been proposed [5]. At this paper it was considered the IC algorithm [4] in order to reach the MPP operational point by a non-inverter buck-boost DC-DC power converter topology.

III. DC-DC State-Space Modeling

The DC-DC converters are used to convert an unregulated DC input voltage into a regulated one. These converters are widely used for DC motors speed control, power supplies and distributed (or stand-alone) generation systems. There are several topologies of them and their main dynamical characteristics are well known [6].

The selection of the circuit topology relies on the power generation plant requirements. At this paper it was evaluated the non-inverter Buck-Boost configuration due to its output voltage characteristic of both decrease (Buck characteristic) and increase (Boost characteristic) it depend on the duty cycle and without polarity inversion during the operation at Continuous Conduction Mode (CCM). The Figure 2 shows both operational states related to non-inverter Buck-Boost DC-DC converter. The paths of main currents are highlighted in red.

As it can be seen at Figure 2, any switch remains (always) neither open nor closed during both operational states. Unlike two of them always share a state in common. As switches S1 and S2 are controlled by the same gate signal, these switches always remain with the same state: open or closed. Likewise, diodes D1 and D2 are both directly or reversely polarized.

The state-space variables presented in (1) are the inductor current, i_{lm} and the capacitor voltage, v_c and the output variable is the load voltage, v_o [6].

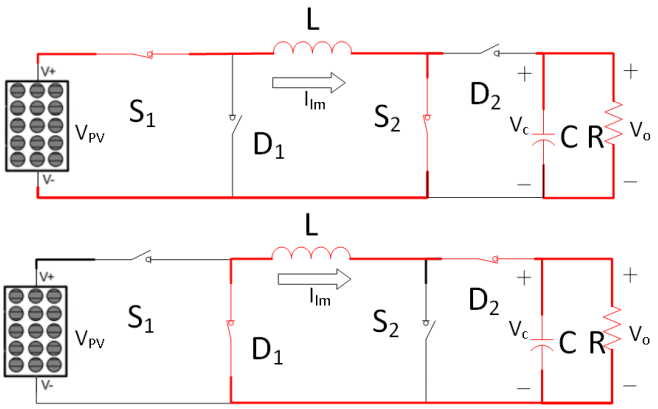

Figure 2.Non-inverter Buck-Boost DC-DC converter operational states.

$$\begin{bmatrix} x \\ y \end{bmatrix} = \begin{bmatrix} \begin{bmatrix} x_1 \\ x_2 \end{bmatrix} \\ [y] \end{bmatrix} = \begin{bmatrix} \begin{bmatrix} i_{lm} \\ v_c \end{bmatrix} \\ [v_o] \end{bmatrix} \quad (1)$$

During each driving range the circuit is described by its state vector, $\boldsymbol{x}$. In order to describe an average behavior of the circuit during the roll switching period, the state equations for the switches ON ($0<t<t_{on}$) and switches OFF ($t_{on}<t<T$) can be expressed by (2) and (3),

$$\dot{\boldsymbol{x}} = [\boldsymbol{A_{on}}\delta + \boldsymbol{A_{off}}(1-\delta)]\boldsymbol{x} + [\boldsymbol{B_{on}}\delta + \boldsymbol{B_{off}}(1-\delta)]v_{pv} \quad (2)$$

$$\boldsymbol{y} = [\boldsymbol{C_{on}}\delta + \boldsymbol{C_{off}}(1-\delta)]\boldsymbol{x} + [\boldsymbol{D_{on}}\delta + \boldsymbol{D_{off}}(1-\delta)]v_{pv} \quad (3)$$

where v_{pv} is the generator terminal voltage, δ is the switching duty cycle, T is the total commutation period and matrices **A-B-C-D** are the state matrices for both conduction cycles of non-inverter Buck-Boost converter [7].

IV. Voltage Control Strategy

Once we have the state-space model of the power converter and the dynamics of the system is known, the next issue is design a control system in closed loop. Due to the robustness of the full state feedback control considering reference input and integral action, the state feedback has been chosen to carry out the drive control of the converter. The control strategy requirements are as follows:

- The matrices **A** and **B** must be controllable;
- The system must not contain poles in origin (s-plane), once the integral action would not be necessary; and

- The system must not contain zeros in origin (s-plane), once the integral action would be canceled.

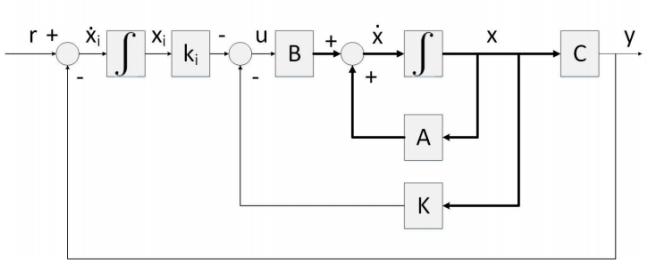

Figure 3. Stead-Space feedback closed loop control with reference input and integral action.

reference input, r. This new state x_i is calculated from the error between signals r and system output (y). The system dynamics now relies on (4) and (5) with **D** null.

$$\dot{\boldsymbol{x}}_{\boldsymbol{a}} = \boldsymbol{A}_{\boldsymbol{a}}\boldsymbol{x}_{\boldsymbol{a}} + \boldsymbol{B}_{\boldsymbol{r}}r \quad (4)$$

$$y = \boldsymbol{C}_{\boldsymbol{a}}\boldsymbol{x}_{\boldsymbol{a}} \quad (5)$$

where $\mathbf{B_r}$ is a column vector with the same size of the steady states variable number plus 1 and $\mathbf{A_a}$, $\mathbf{B_a}$ and $\mathbf{C_a}$ are augmented matrices of the closed loop system given respectively by (6), (7), (8) and (9).

$$\boldsymbol{B}_{\boldsymbol{r}} = [\mathbf{0} \quad \mathbf{0}\cdots\mathbf{0} \quad \mathbf{1}]^{\boldsymbol{T}} \quad (6)$$

$$\boldsymbol{B}_{\boldsymbol{a}} = \boldsymbol{B}^{\circ} = \begin{bmatrix}\boldsymbol{B}\\ 0\end{bmatrix} \quad (7)$$

$$\boldsymbol{C}_{\boldsymbol{a}} = \boldsymbol{C}^{\circ} = [\boldsymbol{C} \quad 0] \quad (8)$$

$$\boldsymbol{A}_{\boldsymbol{a}} = \begin{bmatrix}\boldsymbol{A}-\boldsymbol{B}\boldsymbol{K} & -\boldsymbol{B}\boldsymbol{K}_{\boldsymbol{i}}\\ -\boldsymbol{C} & \mathbf{0}\end{bmatrix} = \boldsymbol{A}^{\circ} - \boldsymbol{B}^{\circ}\boldsymbol{K}_{\boldsymbol{a}} = \\ = \begin{bmatrix}A & 0\\ -C & 0\end{bmatrix} - \boldsymbol{B}^{\circ}\boldsymbol{K}_{\boldsymbol{a}} \quad (9)$$

where $\mathbf{K_a}$ is the feedback state coefficients vector, which can be defined by Ackermann's technique for closed loop pole placement using the $\mathbf{A}^{\circ}$ and $\mathbf{B}^{\circ}$ matrices.

Figure 4 shows the block diagram of the control system proposed for the converter. The $\tilde{\delta}$ represents the small signal perturbation at the duty cycle and $\mathbf{B_d}$ matrix is given by (10).

$$\boldsymbol{B}_{\boldsymbol{d}} = (\boldsymbol{A}_{\boldsymbol{on}} - \boldsymbol{A}_{\boldsymbol{off}})\boldsymbol{x} + (\boldsymbol{B}_{\boldsymbol{on}} - \boldsymbol{B}_{\boldsymbol{off}})v_{pv} \quad (10)$$

It is also important to note that the input v_{pv} is treated as an external disturbance and is not part of the closed loop system, so the poles allocation design is made with $\mathbf{B_d}$ instead of **B**.

V. CONTROL SYSTEM DESIGN

Since the photovoltaic generation systems are susceptible to output voltage changes due to environmental conditions, it is very important that the DC-DC converter control scheme has a fast response capability. Furthermore, it is desirable that those systems have minimum overshooting in order to reducing components stress and increasing lifespan.

Figure 3 shows the block diagram of the proposed control strategy with **D** null. As can be seen at Figure 3, it was added a new state, x_i, as well as the integral constant k_i and the

In addition, an important consideration in the design of DC-DC converter operating on CCM is that the components must ensure the operation in the desired manner, that is, the inductor must be able to smooth the derivative of the current so it does not reach zero anytime. As well the converter output voltage, it is desirable to have minimum ripple. Therefore, the chosen capacitor must be able to handle it.

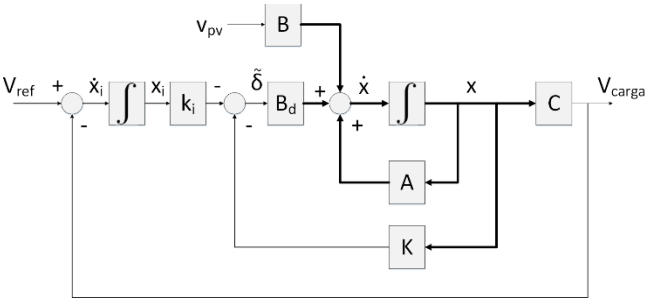

Figure 4. Block diagram of steady-space control method related to DC-DC power converters.

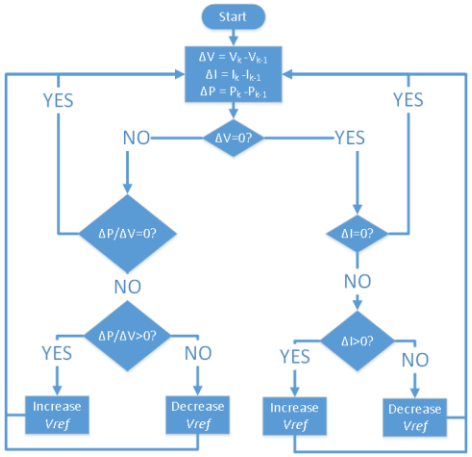

Figure 5. Incremental Condutance (IC) algorithm flowchart.

TABLE I. CIRCUIT ELEMENTS AND PROJECT REQUIREMENTS

Overshooting (%)		*Rising Time (ms)*		
0.02		0.1		
V_{pv} (V)	L (mH)	C (µF)	rc (mΩ)	rl (mΩ)
192	300	5000	10	10
Pole Placement				
-400± j202.2		-400 ± j0		

Table I shows the chosen values for the elements of the circuits that meet the design specifications for operation in the

CCM, made the system controllable and the fits the project requirements.

By set the poles according the values of Table I, the state feedback vector resulted by Ackermann's is given by (11).

$$\boldsymbol{K_a} = [0.0006 \quad 0.0033 \quad -0.6381] \tag{11}$$

VI. MPPT IC ALGORITHM

In order to test the non-inverter buck-boost converter under MPPT conditions the IC algorithm is applied to the power plant. Figure 5 shows the IC algorithm flowchart.

The tracking algorithm comes down to compare the incremental conductance with actual conductance in order to reach the MPP operating voltage value. The IC can reach quickly and accurately the MPP since it no longer changes the operating point once reached. Any change in power forces the algorithm to restart the maximum point tracking [4].

In real applications of the IC algorithm the zeros targets are replaced by some acceptable range instead of crisp values to avoid bounce. Therefore, anything above some defined target or inside some range is taken as target reached. (12), (13) and (14) give the acceptable ranges set in this paper for the IC algorithm.

$$\Delta Ipv_{min} > I_{sc} * 10^{-6} \tag{12}$$

$$|\Delta Vpv_{min}| < V_{oc} * 10^{-6} \tag{13}$$

$$\Delta ICpv_{min} > {\Delta Ipv_{min}}/{\Delta Vpv_{min}} \tag{14}$$

where ΔIpv_{min}, ΔIpv_{min} and $\Delta ICpv_{min}$ are the minimum values for the current, voltage and incremental conductance output PV derivate respectively, I_{sc} is the short circuit current and V_{oc} the open circuit voltage of the array.

The MPPT voltage update rate must be slower than the control algorithm in order to stabilize the PV output voltage. Figure 6 shows the Grid-tie PV system with MPPT schema considered at this papers.

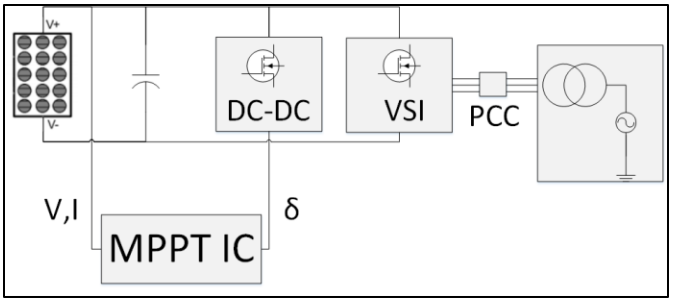

Figure 6. Grid-tie PV system with MPPT schema.

VII. SIMULATION AND RESULTS

After designing control system scheme, the model has been tested in PSCAD. The proposed control strategy was analyzed considering its dynamic response from voltage and load steps. Figure 7 shows the current and voltage output as well the duty cycle of the non-inverter Buck-Boost converter under a value of 384V to voltage reference input.

The analysis of output voltage presented in Figure 7 shows that the steady-state error achieved a minimum value (less than 1%). Besides, the rising time and the overshooting were also closed to desirable conditions.

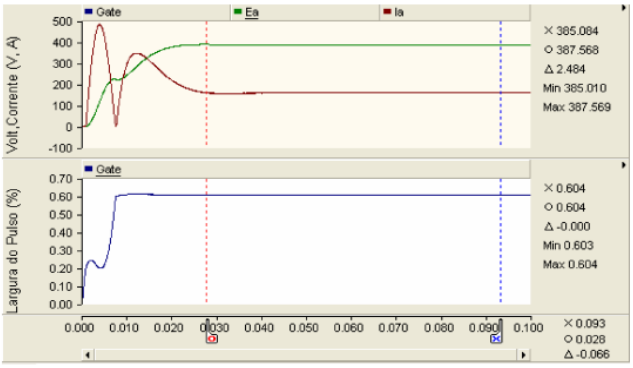

Figure 7. Output voltage control of non-inverter Buck-Boost converter: output voltage (green); output current (red); and duty cycle (blue).

In order to verify the control system sensitivity to load variations, it was applied load steps simulating real conditions of photovoltaic systems operation. The values and the time at which the steps were applied can be seen in Table II.

TABLE II. LOAD STEPS

Load (kW)	Simulation time (s)
20.25	0.00
147.45	0.05
14.74	0.10
20.25	0.15

Figure 8 shows the simulation results considering load steps presented in Table II.

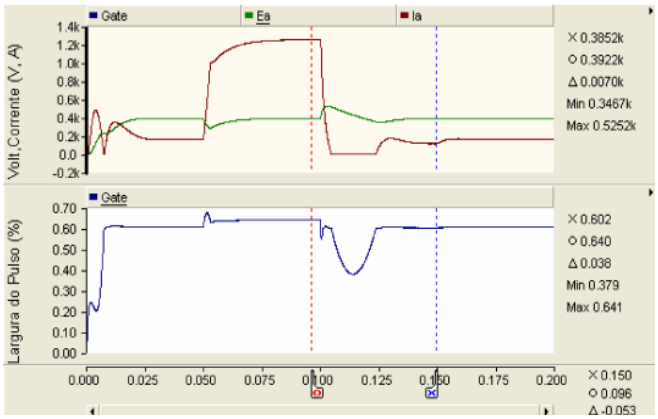

Figure 8. Voltage output control scheme considering load steps: output voltage (green); output current (red); and duty cycle (blue).

By Figure 8, it can be noticed that voltage output reference has been kept closed to the reference input even after applying the load steps. In other words, the control system is able to support abrupt load variations with a rapid convergence and small steady state error.

At this moment, the influence of parasitic resistances in the performance of the control system and its sensitive to parameters variations were considered. The resistances were despised and the inductance value has been decreased by a factor of 10. For the same load steps presented in Table II, the next simulation results are shown in Figure 9.

Figure 9. Voltage control sensibility of parasite resistances and inductance: output voltage (green); output current (red); and duty cycle (blue).

As can be seen at Figure 9, the voltage error was null when the parasitic resistances were removed. This fact confirms the importance of consider the parasitic resistances to system and its model under state-spaces variables method.

Another issue analyzed by simulation model was the capability of the system to track the MPP in photovoltaic arrays. The PV power plant has been simulated based at a distribution grid. The assumed PV array consists of 20 strings in parallel with 20 PV modules in series. The PV array parameters used can be seen at Tables III.

TABLE III. PV ARRAY PARAMETERS

Parameters	Values
No. of modules connected in series / array	20
No. of module strings in parallel / array	20
Number of cells connected in series / module	108
Number of cell strings in parallel / module	4
Reference irradiation	1000
Reference cell temperature	25

The control system has been designed in a way that the MPPT responds slowly than the dynamic of DC-DC converter in order to compensate the converter settling time. The reference voltage update is 10 times slower than the converter settling time designed. Figure 10 shows the implementation of the IC algorithm at PSCAD.

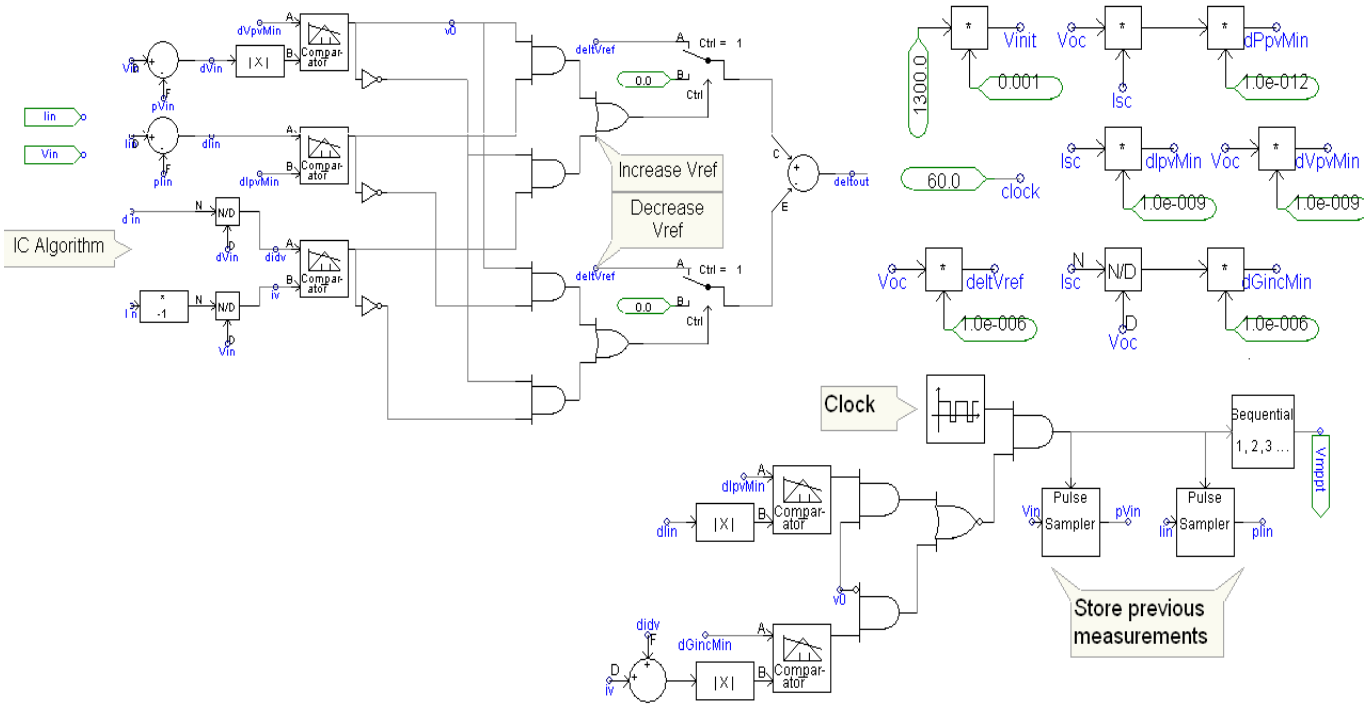

Figure *10*.Implementation of the IC algorithm at PSCAD.

Figure 11 and Figure 12 show simulation results for three conditions of solar irradiance: 1.0, 1.2 and 0.8 kWh/m², respectively. The cell temperature is fixed at 50°C.

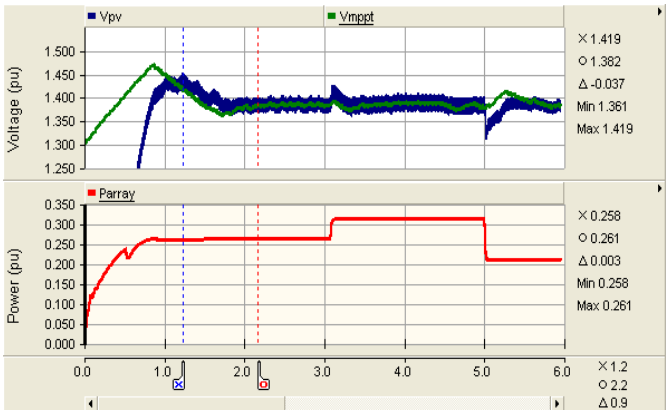

Figure 11. Output PV voltage control using non-inverter Buck-Boost converter under MPP: PV output voltage (blue); MPPT output reference voltage (green); PV output power (red).

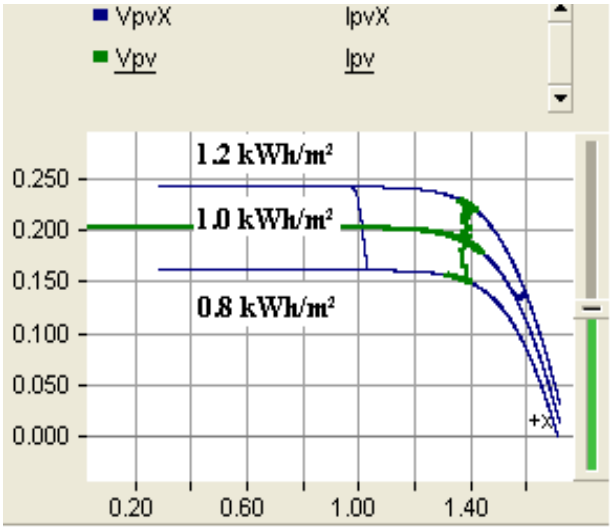

Figure 12. PV power plant operating at MPP: PV output voltage (green), PV I-V curve for diferent solar irradiance levels (blue).

As can be seen at Figures 11 and 12 the DC-DC converter reacted quickly to small reference voltage steps resulting from the MPPT algorithm and was able to track the reference voltage.

VIII. CONCLUSIONS

This paper presents a control strategy for photovoltaic generation systems connected to the grid utility. The system were tested by a PSCAD/EMCT model in order to validate the proposals of this work. The steady-space closed loop feedback control with integral action applied in non-inverter Buck-Boost DC-DC converter can be applied to control the output voltage of this topology. The control technique results on a minimum overshooting and a fast rising time even in high demand variations situations. In addition, the analysis show that the non-inverter Buck-Boost converter considered can be used with a MPPT algorithm in order to maximize output power in PV power generation systems.

REFERENCES

[1] H. G. Beyer, et. al., "Assesing satellite derived irradiance information in south America within the unep resource assessment project swera,"*Proceedings of 5th ISES European Solar Conference in Freiburg*,2004.

[2] WOOFENDEN, I. "Photovoltaic cell, module, string, array", *Home Power*, 113:106- 107, 2006.

[3] Ozuna, G., Anaya, C. Figueroa, D. Pitalua, N. "Solar Tracker of Two Degrees of Freedom for Photovoltaic Solar Cell Using Fuzzy Logic", *Proceedings of the World Congress on Engineering* 2011 Vol II WCE 2011, July 6 - 8.

[4] M. A. GOMES DE BRITO, L. GALOTTO, J. L. P. S. G. D. A. E. M.; C ANESIN, C. A., "Evaluation of the main mppt techniques for photovoltaic applications", *IEEE TRANSACTIONS ON INDUSTRIAL ELECTRONICS*, 60:1156-1167, 2013.

[5] Mohamed A. Eltawila and Zhengming Zhaob, "MPPT techniques for photovoltaic applications"*Renewable and Sustainable Energy Reviews*, vol. 25, pgs. 793–813, 2013

[6] N. Mohan, T. M. Undeland, W. P. Robbins, *Power Electronics: Converters, Applications and Designs*, Jonh Wiley & Sons Inc., New York, NY, 1989.

[7] R.R de C. Vaz. "Análise de Sistema Fotovoltaico de Geração Distribuída Utilizando PSCAD". Monograph of end course project (Electrical Engineering). School of Electrical, Mechanical and Computer Engineering of Federal University of Goiás (UFG), 2014.